International Journal of Pharmaceutics 437 (2012) 1–10

Contents lists available at SciVerse ScienceDirect

International Journal of Pharmaceutics

journal homepage: www.elsevier.com/locate/ijpharm

Understanding reflection behavior as a key for interpreting complex signals in FBRM monitoring of microparticle preparation processes

Kerstin Vay[a,*], Wolfgang Frieß[b], Stefan Scheler[a]

[a] Sandoz GmbH, Sandoz Development Center Austria, Biochemiestrasse 10, A-6250 Kundl, Austria
[b] Department of Pharmacy, Pharmaceutical Technology and Biopharmaceutics, Ludwig-Maximilians-Universitaet Muenchen, D-81377 Munich, Germany

ARTICLE INFO

Article history:
Received 24 May 2012
Accepted 30 July 2012
Available online 4 August 2012

Keywords:
Focus beam reflectance measurement
Microspheres
Particle size analysis

ABSTRACT

The application of focused beam reflectance measurement (FBRM) was studied in a larger scale PLGA microparticle preparation process for monitoring changes of the particle size and the particles' surface properties. Further understanding how these parameters determine the chord length distribution (CLD) was gained by means of single object measurements and data of monodisperse microparticles. It was evaluated how the FBRM signal is influenced by the surface characteristics of the tested materials and the measuring conditions. Particles with good scattering properties provided comparable values for the CLD and the particle size distribution. Translucent particles caused an overestimation of the particle size by FBRM, whereas the values for transparent emulsion droplets were too low. Despite a strong dependence of FBRM results on the optical properties of the samples, it is a beneficial technique for online monitoring of microparticle preparation processes. The study demonstrated how changing reflection properties can be used to monitor structural changes during the solidification of emulsion droplets and to detect process instabilities by FBRM.

1. Introduction

Since the launch of the PAT initiative by the American Food and Drug Administration (FDA) in 2002 in-process measuring methods have become more and more important for manufacturers of pharmaceuticals. The PAT strategy relies on a thorough understanding of the whole manufacturing process and requires predictive relationships between product properties during intermediate process steps and the final product quality. Thus online monitoring methods have become increasingly interesting.

In case of the preparation of biodegradable polymeric microspheres for sustained drug release, the particle size is a decisive factor for their release behavior (Qi et al., 2010; Nilkumhang and Basit, 2009). If such particles are prepared by an emulsion/solvent removal process the size of the resulting microspheres is determined by the droplet diameter of the primary emulsion. In the course of further processing the droplet size undergoes secondary changes which depend, via various mechanisms, on the process parameters of the solvent extraction/evaporation step, for example the stirring rate (Conti et al., 1995; Barkai et al., 1990; Tamilvanan and Sa, 1999). At-line measurements of the microsphere or droplet size are usually accomplished with laser-based particle size analyzers (Jeyanthi et al., 1996; Maa and Hsu, 1997) or the coulter principle (Sansdrap and Moes, 1993; Berkland et al., 2001).

An ideal technique for in-process monitoring of manufacturing the process should be non-destructive and fast enough to allow real-time tracking of the particle or droplet size, respectively. There are several particle sizing methods for in- and online applications based, for example, on laser diffraction (Harvill et al., 1995), ultrasonic attenuation spectroscopy (Babick and Ripperger, 2004; Richter et al., 2007) or phase Doppler anemometry (Black et al., 1996). A preferably used technique for process monitoring is the focused beam reflectance measurement (FBRM) (Zidan et al., 2010). An advantage of this measuring principle is the large particle size range from 1 to approximately 4000 μm depending on the rotating speed of the laser beam. Core piece is a probe, emitting a rotating laser beam, which is mounted in a pipe or dipped into a stirred medium. The laser beam with a wavelength of 780 nm revolves with high velocity of 2–8 m/s depending on the chosen mode, so that the particles' own motion is negligible. When the focus of the laser beam passes a particle, the light is scattered back to the probe window, where the detector is located. The signal is processed by a discrimination circuit with a selectable threshold level. A chord length is calculated from the period during which the light is backscattered to the detector and the speed of the revolving laser beam. Because the radius of the beam's revolution is much larger than the particle diameter, the chord length can be approximated by the length of a straight line between the two points at which the laser beam randomly intersects the boundary line of the particle's

* Corresponding author. Tel.: +43 5338 200 2835; fax: +43 5338 200 2069.
E-mail address: kerstin.vay@sandoz.com (K. Vay).

0378-5173/$ – see front matter © 2012 Elsevier B.V. All rights reserved.
http://dx.doi.org/10.1016/j.ijpharm.2012.07.072

projected area. The FBRM is applicable within a wide concentration or viscosity range and, as up to 100,000 chord lengths are measured per second, statistically robust chord length distributions (CLD) are obtained. However such CLDs are difficult to compare with results of common particle sizing methods because they represent a superimposition of the size distribution of all measured particles and the lengths distribution of all possible chord lengths of each single particle. For example, from monodisperse spheres a chord length distribution can be obtained for which the probability $P_k(x)$ of a chord to lie within an interval from $x-w$ to $x+w$ is

$$P_k(x) = \frac{\sqrt{D_k^2-(x-w)^2} - \sqrt{D_k^2-(x+w)^2}}{D_k}$$

with D_k being the sphere diameter. In a polydisperse particle distribution D_k is the middle of the kth diameter band and w is half the width of the diameter band. The total number of chord size detections at a certain size x ($n(x)$) is the sum of the probability-weighted number of particles in the kth diameter band (n_k):

$$n(x) = \sum_{k=1}^{K} n_k P_k(x)$$

k is the number of bands into which the size range is divided. In order to restore the particle size distribution (PSD) from the CLD the equation has to be solved for n_k. Several methods are available to accomplish this. Calculation is easiest in case of spherical particles. However, if the particle geometry is known it is often possible to convert also CLDs from non-spherical particles into PSDs. This transformation has been subject of several studies (Simmons et al., 1999; Monnier et al., 1996; Sparks and Dobbs, 1993).

Typical applications of FBRM are process optimization, control of crystallization processes (bu Bakar et al., 2009; Chen et al., 2009), polymorphic transformations (Howard et al., 2009; Jia et al., 2008) or the characterization of plant suspension cultures (McDonald et al., 2001). Furthermore several studies using the FBRM for investigation of emulsion systems (Turner et al., 2009; Dowding et al., 2001) were published.

In many of these applications the signal pattern measured by FBRM does not only reflect the geometric characteristics of a CLD as explained above but is strongly biased by additional factors. Especially in case of emulsion droplets and other smooth or transparent particles a marked effect of reflection phenomena becomes apparent. In many cases FBRM data are more dependent on the particles' optical properties than those of other particle sizing methods (Ruf et al., 2000). However most of the previous studies failed to consider these effects. This is also true for the so far only study which describes the use of FBRM in order to monitor a solvent extraction process for microparticle preparation (Zidan et al., 2010). Our work also addresses the application of FBRM in a solvent removal process but puts special emphasis on reflection phenomena affecting the measurement. Deeper knowledge of this issue could broaden the field of possible applications and help to avoid misinterpretations. The study also investigates how this technique can be used in order to monitor alterations of the particles' surface and the interior of transparent particles even if they do not involve any changes of size or shape.

2. Materials and methods

2.1. Materials

Transparent polystyrene research particles (98.7 ± 1 μm) and black polystyrene microspheres (103.9 μm) were obtained from Microparticles GmbH (Berlin, Germany).

Poly (D,L-lactide-co-glycolide) 75:25 (Resomer 755 S): Mw = 64,710 Da was purchased from Boehringer Ingelheim (Ingelheim, Germany). Methylene chloride analytical grade was obtained from Merck (Darmstadt, Germany), and TRIS (Tris(hydroxymethyl)-aminomethan) from AppliChem (Darmstadt, Germany). 3-{2-[4-(6-Fluor-1,2-benzisoxazol-3-yl)piperidono]ethyl}-2-methyl-6,7,8,9-tetrahydro-4H-pyrido[1,2-a]pyrimidin-4-on was purchased from Jubilant Organosys (Mysore, India) and PVA 18-88 from Kuraray Europe GmbH (Frakfurt, Germany).

2.2. Microparticle preparation

Plain microparticles were prepared by an emulsification solvent extraction/evaporation technique. 4.8 g PLGA were dissolved in 46.1 g of methylene chloride and the solution was emulsified in 500 ml of the extraction medium consisting of an aqueous solution of 0.5% (w/v) povidon and 0.1 M Tris buffer (pH 9.0). For the purpose of the droplet size measurements this emulsion was pumped through a flow through cell.

Microparticle preparation started with feeding the emulsion into a 5 l jacketed glass reactor containing 3.5 l of the aqueous phase. By stirring for 5 h the droplets were hardened by solvent extraction and evaporation with an air flow through the headspace of the reactor, which was exactly controlled by a mass flow meter (Vögtlin instruments AG, Aesch, Switzerland). The obtained particles were separated by filtration and dried under vacuum in a desiccator. Different particle batches were produced by varying the extraction temperature between 10 and 35 °C, the air flow through the reactor from 5 to 20 l/min, the stirring speed from 120 to 260 rpm and by adding 0.6% solvent to the aqueous extraction phase. In the same way microparticles containing API were prepared by dissolving 2.8 g 3-{2-[4-(6-fluor-1,2-benzisoxazol-3-yl)piperidono]ethyl}-2-methyl-6,7,8,9-tetrahydro-4H-pyrido[1,2-a]pyrimidin-4-on and 3.2 g PLGA in 46.1 g of methylene chloride.

2.3. Methods

2.3.1. Focused beam reflectance measurement

The FBRM measurements were performed using a Lasentec® D600 FBRM system with a probe for laboratory use (Mettler-Toledo AutoChem, Inc., Redmond, USA). At-line measurements were made at a stirring speed of 400 rpm in a glass beaker using the fixed beaker stand which is an accessory part of the Lasentec® instrument. For this purpose the microparticles were suspended in an aqueous solution of polysorbate 80 (approximately 150 ml) and measured over 5 min. For process monitoring purposes the probe was inserted through the top of the reactor into the stirred suspension (stirring speed 260 rpm), so that the angle of incidence was between 30° and 60°, and the flow was directed obliquely toward the window surface. All measurements were performed using the fine discrimination mode and the default focus position was −20 μm. The FBRM system counts the number of detected chords per second in each size fraction.

2.3.2. Single particle optical sizing (SPOS)

The particle size distributions of polystyrene and PLGA microparticles were additionally measured with an AccuSizer 780 particle size analyzer (Sensor: LE400-05SE; Particle Sizing Systems, Santa Barbara, CA). This instrument uses the principle of light obscuration to count and size particles from 0.5 to 400 μm (single particle optical sensing, SPOS). The data are collected in 512 logarithmically spaced channels with a minimum and maximum fraction width of 1–5.54 μm. Approximately 20 mg of particles were weighed in a sample vessel and suspended in 100 ml of an aqueous solution of polysorbate 80. To ensure a uniform

Table 1
Median of the square weighted CLD and chord- tangent-angle.

Diameter [μm] (micrometer screw)	Median chord length (sqr wt) [μm]	Deviation [%]	Angle α [°]
510	443.8	13.0	60.48
260	204.7	21.3	41.93
240	174.1	27.5	46.50
235	203.0	13.6	59.74
80	66.2	17.3	55.84

suspension, the sample was stirred with a magnetic stirrer and per measurement 50 ml of the suspension was analyzed.

2.3.3. Microscopical image analysis

Microscopical size measurements were performed by the analysis of about 1000 particles per sample using a Nikon eclipse 50i microscope (Nikon Instruments Europe B.V., Kingston, England). The sized particles are classified in size ranges of 2 μm. For every particle size fraction the average volume of a single particle was calculated from the average diameter d_i of each fraction range assuming an ideal spherical shape. By multiplication of the particle count in each fraction with the respective single sphere volume the total volume of each fraction was obtained and a volume weighted particle size distribution was calculated.

3. Results and discussion

3.1. Single object measurements

Techniques, which are based on reflection measurement, can be assumed to be not accurate for particles with strongly convex contours like microspheres. Furthermore as this method is strongly depending on the optical properties, the validity of FBRM should be critically questioned if it is intended to be used for the analysis of reflecting or translucent material. In order to check the quality of the cord length analysis and its suitability for particles with convex surfaces, a simple 2-dimensional system was chosen to investigate the influence of reflecting and curved surfaces on the measured signals. For this purpose thin copper strands with diameters ranging from 80 to 510 μm were attached radially to the sapphire window of the probe. Thus, the laser beam should sweep the copper strand only in the transverse direction. As the strand has the same diameter at each point not a CLD but a single narrow signal peak is obtained. The true diameter of the wires can be easily measured with a caliper or micrometer screw. In contrast to particulate objects, which have shorter chord length at the flanks, the strands have clearly defined diameters. Nevertheless by FBRM values smaller than the true dimensions were obtained.

The median of the chord length differed between 13 and 28% from the true diameters due to the optical surface properties (Table 1). As the surface of the copper strands is smooth and glossy, the laser light is poorly scattered. Because their cross section is not flat, but convex, the intensity of the light which is reflected back to the detector from strongly inclined parts of the surface is below the threshold of detection.

On the basis of these measurements a critical chord-tangent angle α was calculated by computing the arcsine of the quotient of the median chord length (sqr wt) and the diameter determined by the micrometer screw. α ranged from 44° to 60°, beyond which the laser beam is no longer reflected toward the probe head (Fig. 1). The copper strands are an appropriate simplified model to study the FBRM signals obtained from particles with mainly specular or quasi-specular reflection characteristics and convex surfaces. They help to understand the sole influence of reflection phenomena on the FBRM signal, unbiased by chord length effects.

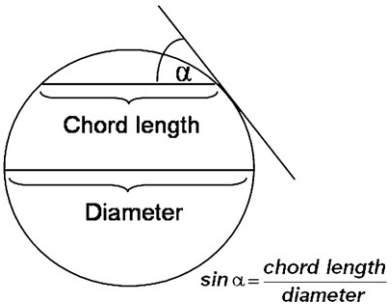

Fig. 1. Cross sectional view of a copper strand: calculation of the chord tangent angle.

3.2. Measurements of monodisperse particle collectives

As a second model, which considers also the fact that from particulate objects chord length distributions rather than uniform values are obtained, monodisperse, spherical polystyrene particles of known size were investigated. The shape of a size distribution is always determined by the weighting method which is employed. Number weighted (called "unweighted" by the Lasentec® software) and square weighted CLDs are chosen below according to the issue being addressed. It is often stated that the square weighted median of the chord length distribution meets best the volume weighted median of the diameter distribution obtained by other particle sizing techniques (Yu and Erickson, 2008; Heath et al., 2002). Also the manufacturer of the Lasentec® device prefers the square weighted median for many applications to be used by default. In order to check this information, the CLD of monodisperse black polystyrene microspheres (⌀ = 103.9 μm) was measured by FBRM and compared with the PSD obtained by SPOS. First monodisperse samples of black polystyrene microspheres with a diameter of 103.9 μm (microscopically sized) were suspended in water (concentration < 1%) and measured in a stirred glass beaker. These results were compared to values obtained by SPOS measurements. The square weighted median of the chord length distribution met best the volume weighted median of the diameter distribution obtained by other particle sizing techniques (Fig. 2). This is in agreement with Heath et al. and consequently in the further course of the work the square weighted CLD or its median is mainly used for comparison with volume weighted PSDs derived from other methods (Heath et al., 2002).

An explanation for this relationship can be found considering the unweighted ([1,0]) and the square weighted ([3,2]) mean chord lengths x_{mean} and x^2_{mean}.

$$x_{mean} = \frac{\sum_{k=1}^{K} f(k) x_k}{\sum_{k=1}^{K} f(k)}$$

$$x^2_{mean} = \frac{\sum_{k=1}^{K} f(k) x_k^3}{\sum_{k=1}^{K} f(k) x_k^2}$$

K is the number of intervals, x_k is the center of the kth interval and $f(k)$ is the probability of measuring a chord included in the kth interval. The terms in the numerators and denominators are the moments of the CLD. As shown by Wynn, E.J.W., the ith moment of the CLD (μ_i) is proportional to the $(i+1)$th moment of the PSD (m_{i+1}) (Wynn, 2003).

$$\mu_i = UTS_i m_{i+1}$$

where U is the speed with which the revolving laser beam progresses, T is the scanning depth, and S_i is a constant dependent on the particle shape. Thus, square weighting of the (unweighted) [1,0]

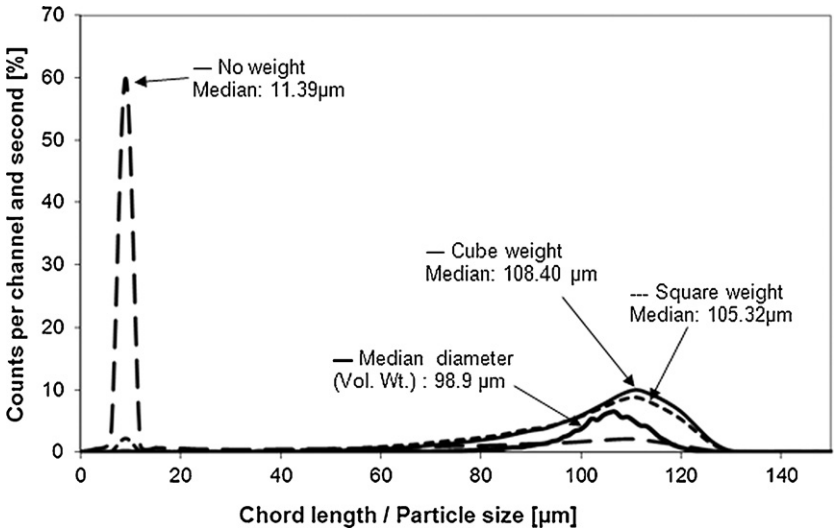

Fig. 2. Effect of various weightings on the median of the chord length distribution of monodisperse black polystyrene microspheres (Ø = 103.9 μm, microscopically sized): unweighted median (dashed line): 11.39 μm, square weighted median (dotted line): 105.32 μm and cube weighted median (solid line): 108.40 μm.

average of the CLD leads to the [3,2] CLD average which, according to the above mentioned equation, is proportional to the [4,3] average of the PSD. Because this volume weighted mean diameter (d[4,3]) is also obtained by laser diffraction, square weighting of the CLD provides a good approximation to those volume-based PSDs.

Surprisingly, in the unweighted distribution shown in Fig. 2 a first peak occurs at a small size of only about 10 μm. This signal can be explained by chord splitting which means that low-amplitude signals are superimposed by the baseline noise thus triggering the analyzer to detect multiple small peaks instead of one large signal (Ruf et al., 2000). Such an artificial chord splitting peak can also be found in case of transparent monodisperse polystyrene microspheres (Fig. 3).

The CLD of the transparent particles shows also another signal without any obvious reference to the particle diameter. This peak at 54 μm can be attributed to specular reflection phenomena. As the particles do not have a flat but a convex shape, their margins are disinclined to the incident laser beam. In case of a smooth particle surface a large proportion of the light is specularly reflected. At a certain surface inclination the reflected ray, which makes the same angle as the incident ray with respect to the surface normal, does no longer pass the probe's aperture. A signal is detected as long as the light cone hits the particle surface in a position which allows at least partial reflection back to the detector. This depends on the beam's divergence angle, the aperture diameter, the distance between aperture and particle surface, the particle size, and its distance to the focus point. It can be shown that these conditions are fulfilled within a 54 μm-section of the focus path in case of 98.7 μm microspheres (Scheler, 2011).

The main peak at 153 μm indicates a chord length which is much larger than the diameter of the spheres. Such large chord lengths can only be caused by divergent rays of the light cone which hit a particle even before the optical axis reaches the particle's outline. However, during this time frame of oblique illumination no substantial reflection toward the detector can be expected if the surfaces have only specular reflecting or Lambertian scattering properties because in these cases angular incident beams are reflected in the opposite direction of the detector (at least if the particles are not in far distance to the probe window). Only in case of internal reflection or subsurface scattering, which occurs if the particles are transparent or translucent, a substantial part of the light flux is reflected or scattered toward the detector for a longer

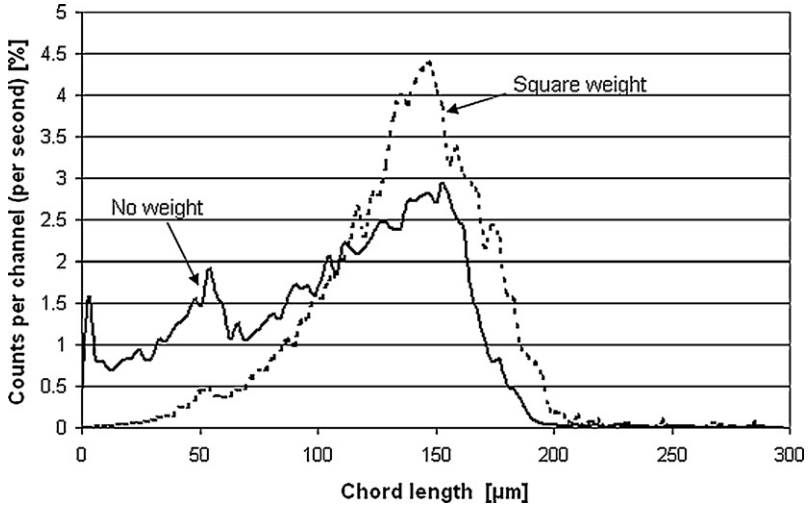

Fig. 3. Optical pathways in case of objects with subsurface scattering (polystyrene microspheres), mixed specular and lambertian (copper strands, emulsion droplets), and lambertian (e.g. PLGA microspheres) scattering properties.

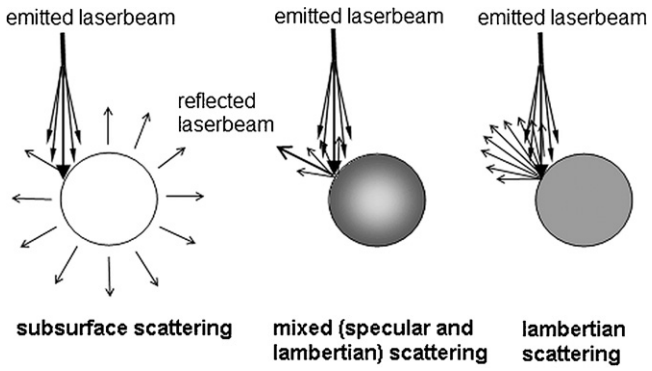

Fig. 4. Unweighted and square weighted chord length distribution of monodisperse transparent polystyrene particles (Ø = 98.7 ±1 μm according to manufacturer's data).

period than the focus point needs to cross the particles projection plane.

If the laser beam hits a translucent particle multiple reflections within the particle occur and the whole sphere lights up (Fig. 4). This effect lasts from the first contact of the light cone with the edge of the particle until the light spot has moved completely off the particle. Thus the duration of the signal is longer than the time span which the focus point itself would need to pass from the one edge to the other and chord lengths larger than the particle diameter are obtained (Fig. 5). Such reflection phenomena can explain the third maximum at 153 μm of the unweighted CLD curve in Fig. 3.

The square weighting of the chord length distribution masks the trimodal distribution pattern resulting in only one broad peak with a median (sqr wt) of 141.1 μm and a square weighted mean of 137.2 μm. By contrast the volume weighted diameter measured by SPOS shows a very narrow distribution with a much smaller mean value of only 98.3 μm. It correlates well with the microscopically obtained mean particle size provided by the manufacturer (98.7 μm) and with measurements from own photomicrographs (98.9 μm) (Fig. 6a). As the data show, there is a considerable deviation between the particle diameter and the chord length values measured by FBRM with the latter being about 40% larger than the true particle size.

In order to prove the assumption that this mismatch is caused by internal reflections, as discussed above, the measurements were compared with non-transparent, black microspheres. The volume weighted median diameter of the black microspheres (Fig. 6b) was measured as 103.9 μm with SPOS and exactly the same value was also found by microscopy. In this case, however, the square

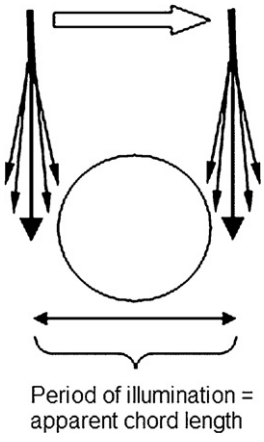

Fig. 5. Illumination time for subsurface scattering and resulting apparent chord length.

weighted median measured with FBRM was found to be 105.0 μm (mean = 98.8 μm), which meets the mean particle diameter much better than observed with transparent particles (Fig. 2). Due to the high absorbance of the black particles, the backscattered signal is only very weak, which results in a high degree of chord splitting recognizable by a huge peak at 10 μm in the unweighted distribution. However, the chord splitting peak becomes nearly insignificant if square weighted data are plotted. This effect is also reflected by the median of the CLD which rises from 11.39 μm to 105.32 μm (unweighted mean: 36.4, square weighted mean: 98.8 μm) when applying the square weighted instead of the unweighted distribution.

Summarizing the aforementioned results, the square weighted mean or median of a chord length distribution is a much better estimate for the mean or median particle diameter than the unweighted statistics. However, it was also shown that FBRM data, regardless by which type of weighting they are obtained, might not represent the true size if transparent or translucent particles are measured.

In contrast to copper strands which are singular objects positioned in a fixed distance (i.e. directly at the probe window) particle suspensions contain a large number of reflecting objects located at varying distances which are hit randomly by the laser beam. Both factors, the particle concentration and their distance from the focus point, affect the detector signal. Depending on their distance to the probe a more or less broadened light spot is projected onto the particles by the divergent beam. As the focus position is displaceable, the cross sectional size of the beam in front of the probe window can be varied, which, in turn, changes the reflection signal. These complex interactions make it very difficult to pre-estimate the effect of these parameters. For this purpose a series of tests was performed to study the influence of these factors.

3.2.1. *Influence of the position of the focal point*

There are different variables which can affect the optimum focus position like the particle size range, the solid concentration of the suspension or the optical properties like the refractive index of the dispersant. For very fine particles best results are usually obtained if the focus is positioned inside the probe window, for larger particles the optimum is found by moving the focus position into the suspension (Sparks and Dobbs, 1993). A generally recommended default setting given by the manufacturer of the Lasentec® instrument is −20 μm, which means, that the focus of the laser beam lies slightly inside the sapphire window. The more the focal point is moved inside the probe window, the more the laser beam is broadened and weakened in front of the window (Worlitschek, 2003). Thus the intensity of the laser beam hitting the particle surface decreases and in turn the backscattered light flux is reduced. This causes a change in the measured particle size because reflection from the tilted peripheral areas of the spheres falls below the detection threshold.

To determine whether a more accurate particle size can be obtained with an optimized focal position, transparent polystyrene particles were measured with varying positions of the focus ranging from −80 to +200 μm. A focus position between −40 and 100 μm showed no significant influence on the unweighted and only a slight influence on the square weighted median chord length (Fig. 7). Only a position of the focal point more than 40 μm inside the probe window produced a sudden and significant drop of the measured particle size. However, neither the unweighted nor the square weighted median of the CLD reached the true particle diameter even at the −80 μm focus position. The focus position seems to be a parameter which has only limited influence on the measured particle size. For this reason the default setting of −20 μm was maintained for all further measurements.

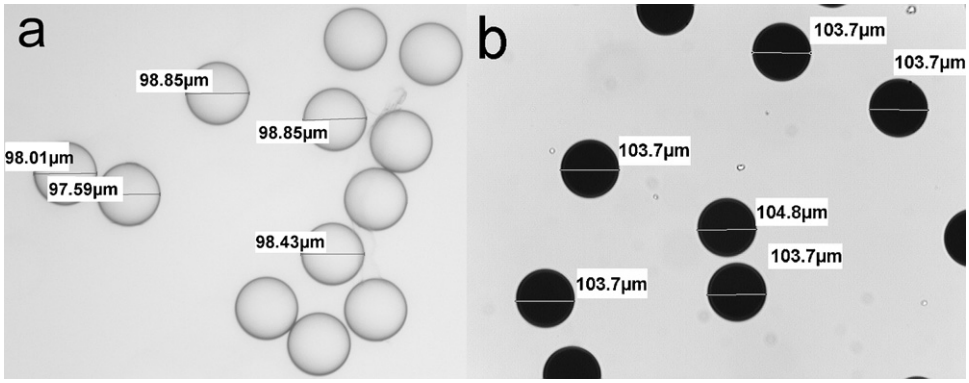

Fig. 6. Photomicrographs of transparent (Ø = 98.7 ± 1 µm) (a) and black (Ø = 103.9 µm) (b) monodisperse polystyrene microparticles.

3.2.2. Influence of the particle concentration

FBRM is a particle sizing method, which is well suited for analysis in suspensions with a high solid concentration. In typical solvent extraction evaporation processes for the preparation of PLGA microparticles the concentration is about 0.2% and thus it is rather low with respect to the range covered by this measuring method. To ascertain whether the method can be used for such applications, low concentrated suspensions with 0.2–3% (m/v) solids were investigated using slightly translucent PLGA microspheres. Despite a volume weighted median of the PSD of 103.2 µm, determined with SPOS, the square weighted median of the CLD (FBRM measurement) ranged between 79.5 and 82.5 µm depending on the particle concentration. The maximum value was found at a solid concentration of 1% (Fig. 8). Above this concentration it decreases marginally, which is in accordance with the findings of Yu et al., who reported, that the square weighted median of the CLD decreases with rising solid concentration of PVC particles (Yu and Erickson, 2008). By analyzing single ceramic beads Ruf et al. constituted that the laser penetration depth is reduced with an increase of the solid concentration and is thus limiting the diameter of the light spot by which the furthermost particles are scanned (Ruf et al., 2000). At a high solid concentration only those particles are detected, which are passing the laser beam in short distance to the probe window, and thus very close to the focal point.

If the particle concentration is low also particles, which are not directly at the probe window are detected. The deeper the laser beam penetrates into the suspension, the more it is widened and the measuring signal is prolonged. For this reason the median of the CLD increases slightly when the solid concentration decreases. In case of very low solid concentrations weak reflections from distant particles cause noisy fluctuations of the detected signal, resulting in chord splitting as described above. This leads to a sharp decline of the square weighted mean at particle concentrations below 1%. Yu et al. could find this behavior only for the unweighted mean but with no effect on the square weighted mean (Yu and Erickson, 2008).

Although the FBRM is applicable for a wide concentration range, its main field of application is the measurement of dispersions with high solid concentrations. As the experiments show, a variation of the concentration from 0.2 to 3.0% does not change the square weighted median chord length by more than 3 µm which is acceptable for the intended application of the method. Considering this low sensitivity to the solids concentration within the range of interest, the method was shown to be also suitable for processes with highly diluted suspensions, e.g. for monitoring of microparticle preparation by emulsion/solvent removal techniques.

3.3. CLDs of heterodisperse particle collectives and emulsion droplets

As mentioned above, microparticles consisting of PLGA are usually slightly translucent depending on type, amount and dispersity of incorporated drug substances. Before using FBRM for in-process monitoring in PLGA-microparticle preparation, it has to be clarified whether the kind of reflectiveness allows for accurate

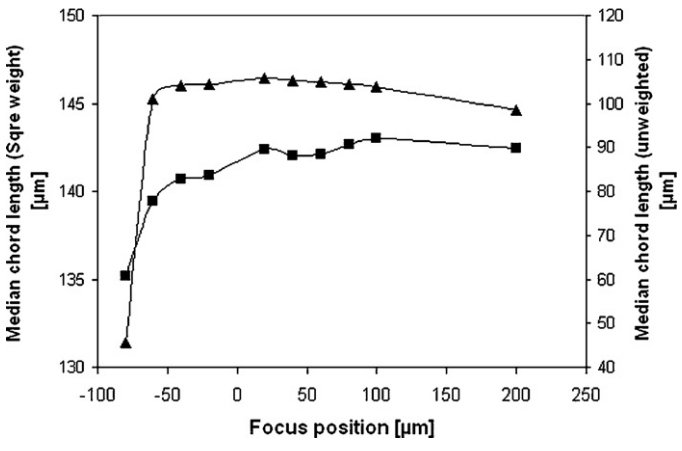

Fig. 7. Influence of the focus position on the unweighted (-▲-) and square weighted (-■-) median of the CLD of transparent monodisperse polystyrene microparticles (⌀ = 98.7 ± 1 µm).

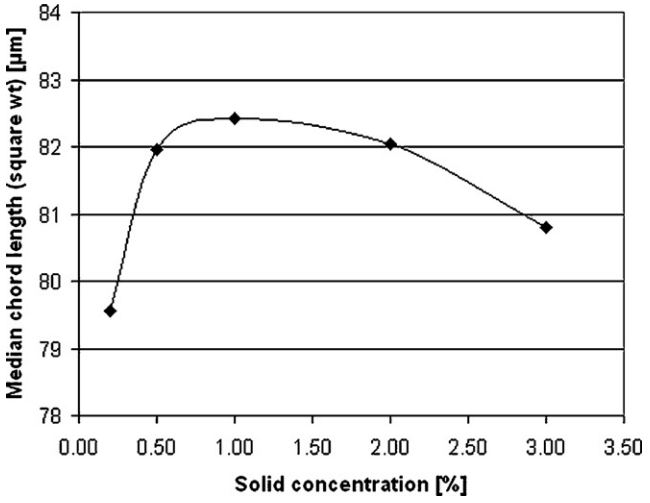

Fig. 8. Correlation between square weighted CLD and solid concentration (% m/v) in suspensions of PLGA microparticles.

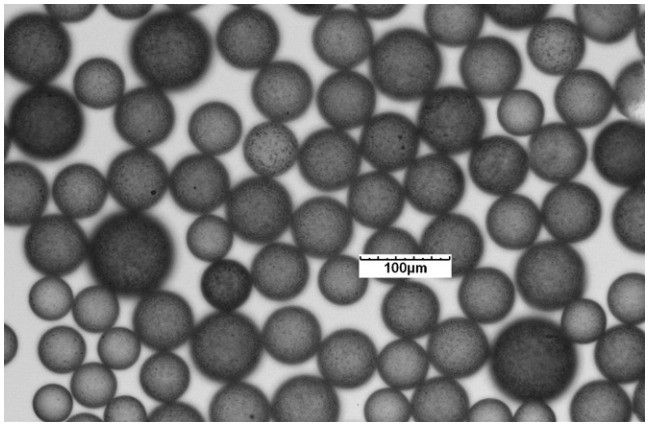

Fig. 9. PLGA placebo microspheres (batch no. 4 (Table 2)).

measurements or whether a high degree of internal scattering distorts the results.

A series of batches of plain and drug loaded PLGA microspheres was produced under different process conditions by varying the stirrer speed and the rate of the head space ventilation. As can be seen by microscopy, all tested PLGA particles have a rougher surface and are much less translucent than PS particles, which leads to the expectation that superficial scattering might be more pronounced than internal scattering or reflection (Fig. 9).

The particle size of the samples was analyzed by FBRM and SPOS. For all types of particles the two methods produced diverging results, with the square weighted median of the CLD (measured by FBRM) being consistently lower than the volume weighted median of the PSD (obtained by SPOS) (Table 2, batches 1–5). Due to the particles' poor transparency, this deviation is mainly caused by non-Lambertian reflection phenomena, most probably by those of a specular type, which were shown above to decrease the measured chord lengths.

Fig. 10 shows, as an example, the cumulative volume weighted PSD and the square weighted CLD of particle batch 2. As indicated by about the same slope of both curves, square weighting is able to transform a CLD into an equally shaped distribution as the PSD. The missing congruence in form of a parallel offset is due to the difference of the medians which is caused by the fact that the particles show also other types of reflection than solely diffuse (Lambertian) surface scattering.

In microparticle manufacturing by a solvent extraction/evaporation process, which is based on the preparation and further processing of a primary emulsion, monitoring of the

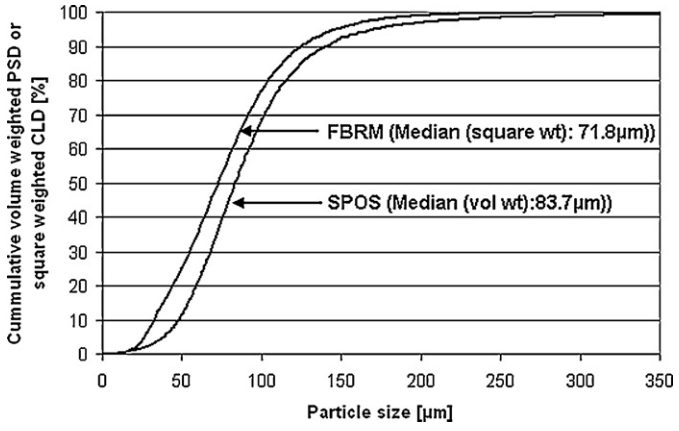

Fig. 10. Cumulative size distributions of PLGA microspheres (batch 2) measured with FBRM and SPOS.

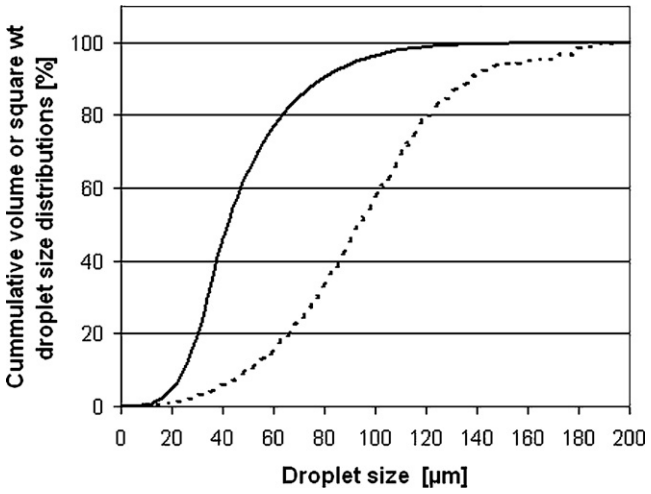

Fig. 11. Comparison of the droplet size distribution measured with FBRM (—) (median (sqr wt): 41.8 µm) and with image analysis by microscopy (- - -) (median (vol wt): 94.7 µm).

initial droplet size and its change in the course of the process can be a valuable tool for development and process control. The determination of the primary emulsion's initial droplet size is a demanding problem as the droplets are transparent and thus FBRM might not provide accurate values. On the other hand the emulsion is too concentrated for undiluted measurement with SPOS. Dilution however causes solvent extraction and in turn changes of the droplet size.

To clarify these problems the emulsion was measured on the one hand with the FBRM probe mounted in a flow through cell at the outlet of the mixer and on the other hand with microscopic image analysis. As expected, due to their transparency the droplets caused only low backscatter to the detector. The square weighted median of the chord length measured with FBRM was 41.8 µm which is only half of the mean droplet size obtained by image analysis (Fig. 11). This demonstrates that FBRM is strongly dependent on the optical properties of the measured specimens and is not an appropriate method to determine the size of transparent emulsion droplets. This is in agreement with Greaves et al. and was also found by Sparks and Dobbs, who concluded that only droplets which are opaque and highly reflective (with microstructure on the surface) give reproducible and accurate results (Greaves et al., 2008; Sparks and Dobbs, 1993).

The unweighted CLD of the emulsion (data not shown) shows again a very high number of small chord lengths, as in the case of the transparent polystyrene microparticles. This indicates again the phenomenon of chord splitting which appears if reflection is weak. Thus, the at-line measurement of the primary emulsion and the finished particles demonstrates that FBRM does not provide reliable values for emulsion droplets. The finished microspheres, however, can be measured in many cases with only small and acceptable deviations.

3.4. Online-monitoring of a microparticle preparation process by FBRM

While FBRM is only of limited use for measuring absolute droplet or particle size distributions, it can nevertheless be an appropriate tool for process monitoring. This was studied with different batches of microspheres which were prepared under conditions with modified solvent extraction from the emulsion droplets, resulting in "rapid" or "slow" hardening of the microspheres. The rate of solvent evaporation has a strong influence on the encapsulation efficiency and on the morphology of the resulting microspheres, which is an

Table 2
Process parameters of PLGA microspheres and CLD, resp. PSD measured by FBRM and SPOS.

Batch no.	API	Air flow [l/min]	Stirring speed [rpm]	FBRM – median sqr wt [μm]	Accusizer – median vol wt [μm
1	–	10	260	39.28	61.43
2	+	10	260	71.8	83.7
3	–	5	220	48.47	58.11
4	–	5	120	36.14	55.04
5	+	5	120	38.25	50.37
6	–	1	220	39.49	56.31

important factor controlling the drug release (Li et al., 1995; Yeo and Park, 2004).

Two batches prepared at 35 °C with different stirring speed and air flow were compared to each other. Fast solvent extraction was obtained at a high stirring speed of 260 rpm and an intensive air flush of 10 l/min through the head of the reactor (batch no. 1). The process parameters for slow extraction were 120 rpm and 5 l/min (batch no. 4) (Table 2). As described above, the FBRM is strongly dependent on the surface properties and the transparency of the measured samples. For this reason different values are obtained from emulsion droplets and equally sized solidified particles. Thus the transition of liquid emulsion droplets into solid microparticles should be accompanied by a significant change of the FBRM signal.

As Fig 12a shows, in case of fast solvent removal the first measurable (artificial) value for the square weighted median is about 28 μm. Within a minute it increases to 40.8 μm (sqr wt median). By contrast, slow solvent extraction produces particles with initial FBRM signals of more than 160 μm. However, within the first 4–6 min of the process the signal drops down to a value of 45 μm, which corresponds to the apparent size of the rapidly extracted particles.

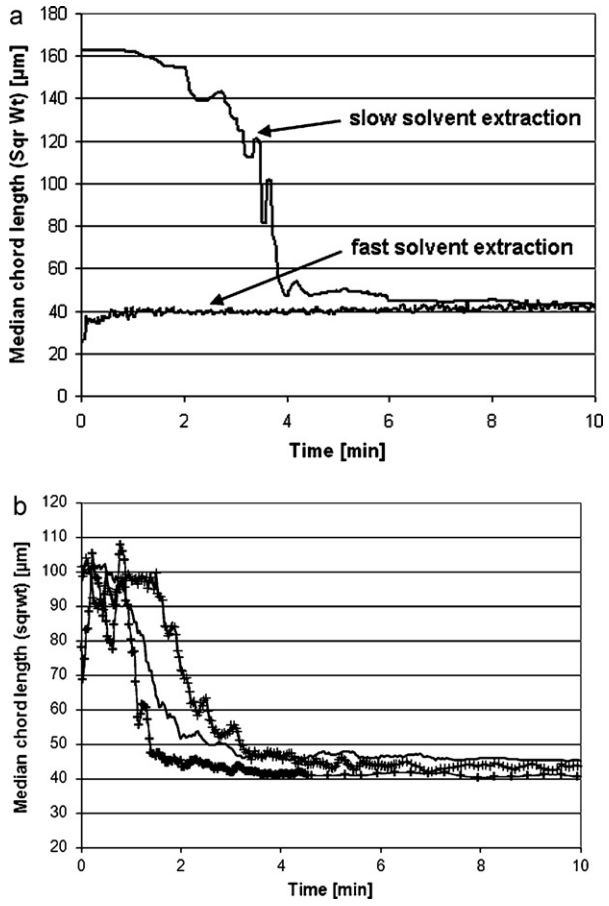

Fig. 12. (a) Droplet, resp. particle size during processing of placebo microparticles with fast (10 l/min, 260 rpm; batch no. 1) and slow (5 l/min, 120 rpm; batch no. 4) solvent extraction and (b) Droplet, resp. particle size of placebo microparticles during processing with solvent extraction at 10 °C (air flow: 20 l/min, stirring speed: 260 rpm) with methylene chloride addition to aqueous phase (- - -) and without solvent in the extraction phase (-+-).

There are also other ways to slow down the solvent extraction rate und thus to affect the product properties, e.g. to apply a low process temperature of only 10 °C. Under these conditions of fast stirring and fast air flush (260 rpm, 20 l/min) but low extraction temperature (10 °C) a significantly higher initial particle size (about 100 μm) than in case of 35 °C and otherwise equal parameters was measured. Again it dropped down to about 45 μm after 1–2 min. Feeding the emulsion droplets into an aqueous phase already containing methylene chloride was tested as an option to decelerate the extraction process. However, the addition of 0.6% of methylene chloride to the aqueous phase did not render a markedly delayed particle formation (Fig. 12b).

It has to be pointed out that the measured size values must not be considered as true particle sizes rather than as FBRM signals which are strongly determined by the optical properties of the particles and thus need a thorough interpretation regarding the information derivable from these data.

The first process, which starts even in the mixer and continues after the emulsion is fed into the extraction tank, is a very fast redistribution of methylene chloride from the droplets into the continuous phase and into the extraction medium. As long as the polymer solution in the droplets is rather diluted solvent removal does not cause any, not even any locally limited phase transition. The droplets remain liquid but lose solvent within seconds and shrink abruptly in size. This step is too fast for monitoring it by FBRM. After the polymer concentration has reached a certain limit the further course of the process is determined by the rate of solvent removal.

In case of fast solvent extraction, the polymer solidifies rapidly on the droplet surface (Freitas et al., 2005), which, as a result, becomes to a certain degree diffusely scattering. This change from solely specular reflecting to partly Lambertian scattering properties is most probably the reason for the apparent increase of the median chord length from about 28 to 40 μm, which can be seen in Fig. 12a. During further processing, water molecules penetrate into the initially solvated polymer matrix and replace the molecules of the organic solvent. The subsequently hydrated, as well as the initially solvated microparticles show a smooth surface with partly diffuse but dominating specular characteristics like in case of the copper strands described above. Thus the value obtained by FBRM is distinctly smaller than the true particle size which was found to be characteristic for specular objects. The square weighted median of about 40 μm remains constant all over the extraction period which indicates, that the optical properties do not change for the entire duration of the process.

In case of slow extraction, during the first 2–4 min the square weighted median is considerably higher than the value which is measured for the primary emulsion. Subsequently, it drops down to a value between 40 and 50 μm which remains nearly constant

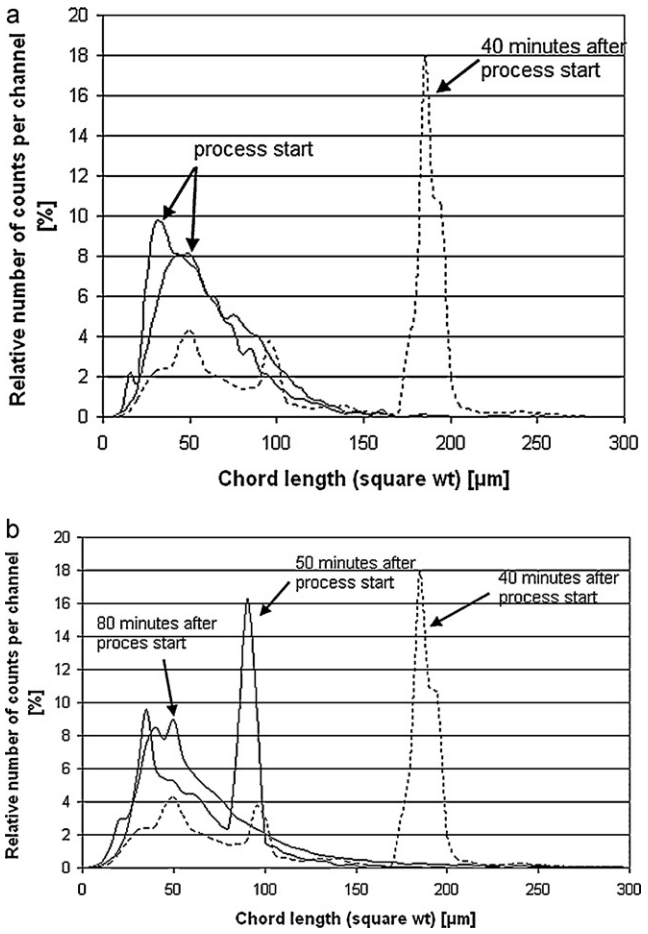

Fig. 13. (a) CLD pattern during processing. CLD at the beginning of the process (—) after delivering the emulsion into the reactor and after 40 min of process duration (- -) of batch no. 5. and (b) Occurrence of crystal needles and shift of the signal peaks during processing (batch 5).

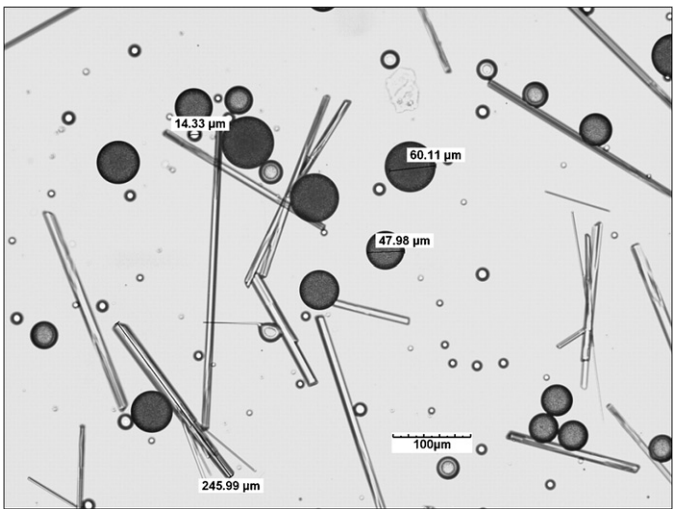

Fig. 14. Crystal needles and microparticles in aqueous phase during processing (batch 5).

until the end of the extraction process. This phenomenon could be observed for all batches with decelerated solvent removal irrespectively of the method by which the extraction rate was decreased. As shown by the preliminary experiments subsurface scattering was identified as the main reason for a significant overestimation of the particle size. Most likely it causes also the apparent droplet expansion immediately after feeding the emulsion into the extraction medium. In case of slow solvent extraction no instantaneous formation of a skin layer on the particle surface is to be expected. Instead segregation processes inside the droplets or embryonic particles are recorded. Due to phase separation the optical properties of the previously transparent emulsion droplets change to opaque. Under the microscope the formation of a granular structure inside the particles can be observed in this phase. After this transitional stage, solidification progresses with a further opacification of the internal particle structure and the formation of a smooth and largely specular surface which both impede the penetration of the laser beam into subsurface regions. The specular reflection behavior causes an underestimation of the particle size as discussed before. Thus the decrease of the FBRM signal has to be assumed not to reflect a size change but rather marks the point where particle solidification occurs.

In all cases the conversion of liquid droplets into solid particles was exceptionally fast. At the latest about 4–6 min after feeding the emulsion into the reactor the square weighted median had reached its final value. This period of the process has therefore the greatest impact on the resulting particle morphology and should be the main target for measures to control the particle properties.

In the preparation of drug loaded PLGA particles another additional phenomenon could be observed by FBRM. In some cases about 40 min after starting the process a high signal peak occurred at a chord length of 185 μm (Fig. 13a). Subsequently this main peak shifted from 185 μm to 90 μm and then a third peak appeared at 35 μm. After another 50 min the peaks disappeared completely (Fig. 13b). After occurrence of the first signal peak a sample was taken and examined microscopically, revealing thin drug crystal needles with a length up to approximately 200 μm.

By encapsulating a high amount of the poorly water soluble active ingredient into polymer particles, the process can get unstable under unfavorable process conditions. If hardening of the microspheres occurs too slowly (batch no. 5, Table 2), the drug substance is not tightly enclosed inside the polymer matrix and can diffuse out of the nascent particles and precipitate in the aqueous phase (Fig. 14). These needle shaped crystals are detected by FBRM and sharp peaks occur representing their longitudinal dimension. In the course of stirring the fragile crystal needles break to pieces and the signal shifts to smaller values. It seems that each fracture results in needles with about half the size of the initial crystals (185 μm → 90 μm → 35 μm).

At a certain time point, the needles are so small, that their signals cannot be distinguished from those of the microspheres.

4. Conclusions

In this work the use of focused beam reflectance measurement for the determination of chord length distributions of spherical microparticles and emulsion droplets and its applicability for monitoring of microparticle preparation processes has been studied.

FBRM data are highly dependent on the material properties of the analyzed samples and were influenced by measuring parameters like the solid concentration in the suspension or the focal point position. Materials with reflective properties due to smooth surfaces are not suitable to be accurately analyzed by FBRM. They tend to provide signals much smaller than their true particle size. By contrast, translucent emulsion droplets usually originate signals mimicking too large particles. However, the size of particles with a rough surface and thus good backscattering properties, like PLGA microspheres, could be well estimated.

In spite of these limitations, FBRM is a strong tool to provide new insights into the microparticle formation in a solvent removal

process. The transformation of the emulsion droplets into solidifying particles can be detected by a change in the FBRM signal. In a solvent extraction/evaporation process based on methylene chloride, solidification of the emulsion droplets and particle size changes occur within the first seconds to minutes after feeding the emulsion into the reactor. These changes cannot be monitored by any at-line particle size measurements. As the FBRM signal is strongly depending on the surface properties of the measured sample, it provides an effective solution to track this process. It is a great advantage of the FBRM, that it requires no sampling and separate analysis. With regard to controlling such a microparticle preparation process the determination of the rate and time point of conversion from liquid droplets to solid particles is of great interest. The solidification rate is an important parameter influencing the encapsulation efficiency and the initial burst in microparticulate systems. A very slow hardening of the emulsion droplets leads to the diffusion of the drug substance out of the droplets and precipitation in the external phase. This event could be monitored by FBRM. For these reasons FBRM is a useful tool to investigate the effect of different process variables, like stirring speed or air flow, on the solidification rate and to assess its influence on the resulting particles and thus can help support a subsequent scale up process. However, unlike conventional applications of FBRM, monitoring of such processes which are accompanied by changes of optical properties requires a thorough understanding of the measuring principle and a deep knowledge of signal generation and processing by the instrument. Basically, FBRM is not a trivial method. In every application the possibility of artifacts due to changes of reflective properties should be considered and results should always be critically questioned.

References

Babick, F., Ripperger, S., 2004. Characterization of concentrated emulsions by means of ultrasonic spectroscopy. Chem. Ing. Tech. 76, 30–40.

Barkai, A., Pathak, Y.V., Benita, S., 1990. Polyacrylate (Eudragit retard) microspheres for oral controlled release of nifedipine.1. Formulation design and process optimization. Drug Dev. Ind. Pharm. 16, 2057–2075.

Berkland, C., Kim, K., Pack, D.W., 2001. Fabrication of PLG microspheres with precisely controlled and monodisperse size distributions. J. Control. Release 73, 59–74.

Black, D.L., Mcquay, M.Q., Bonin, M.P., 1996. Laser-based techniques for particle-size measurement: a review of sizing methods and their industrial applications. Prog. Energy Combust. Sci. 22, 267–306.

bu Bakar, M.R., Nagy, Z.K., Rielly, C.D., 2009. Seeded batch cooling crystallization with temperature cycling for the control of size uniformity and polymorphic purity of sulfathiazole crystals. Org. Process Res. Dev. 13, 1343–1356.

Conti, B., Genta, I., Modena, T., Pavanetto, F., 1995. Investigation on process parameters involved in polylactide-co-glycolide microspheres preparation. Drug Dev. Ind. Pharm. 21, 615–622.

Chen, J.X., Yuan, J.S., Ulrich, J.C., Wang, J.K., 2009. Online measurement of hydrocortisone particles and improvement of the crystallization process. Chem. Eng. Technol. 32, 1073–1077.

Dowding, P.J., Goodwin, J.W., Vincent, B., 2001. Factors governing emulsion droplet and solid particle size measurements performed using the focused beam reflectance technique. Colloids Surf. A: Physicochem. Eng. Asp. 192, 5–13.

Freitas, S., Merkle, H.P., Gander, B., 2005. Microencapsulation by solvent extraction/evaporation: reviewing the state of the art of microsphere preparation process technology. J. Control. Release 102, 313–332.

Greaves, D., Boxall, J., Mulligan, J., Montesi, A., Creek, J., Sloan, E.D., Koh, C.A., 2008. Measuring the particle size of a known distribution using the focused beam reflectance measurement technique. Chem. Eng. Sci. 63, 5410–5419.

Harvill, T.L., Hoog, J.H., Holve, D.J., 1995. In-process particle size distribution measurements and control. Part. Part. Syst. Char. 12, 309–313.

Heath, A.R., Fawell, P.D., Bahri, P.A., Swift, J.D., 2002. Estimating average particle size by focused beam reflectance measurement (FBRM). Part. Part. Syst. Char. 19, 84–95.

Howard, K.S., Nagy, Z.K., Saha, B., Robertson, A.L., Steele, G., Martin, D., 2009. A process analytical technology based investigation of the polymorphic transformations during the antisolvent crystallization of sodium benzoate from IPA/water mixture. Cryst. Growth Des. 9, 3964–3975.

Jia, C.Y., Yin, Q.X., Zhang, M.J., Wang, J.K., Shen, Z.H., 2008. Polymorphic transformation of pravastatin sodium monitored using combined online FBRM and PVM. Org. Process Res. Dev. 12, 1223–1228.

Jeyanthi, R., Thanoo, B.C., Metha, R.C., Deluca, P.P., 1996. Effect of solvent removal technique on the matrix characteristics of polylactide/glycolide microspheres for peptide delivery. J. Control. Release 38, 235–244.

Li, W.I., Anderson, K.W., Mehta, R.C., Deluca, P.P., 1995. Prediction of solvent removal profile and effect on properties for peptide-loaded PLGA microspheres prepared by solvent extraction/evaporation method. J. Control. Release 37, 199–214.

Maa, Y.F., Hsu, C.C., 1997. Effect of primary emulsions on microsphere size and protein-loading in the double emulsion process. J. Microencapsul. 14, 225–241.

McDonald, K.A., Jackman, A.P., Hurst, S., 2001. Characterization of plant suspension cultures using the focused beam reflectance technique. Biotechnol. Lett. 23, 317–324.

Monnier, O., Klein, J.P., Hoff, C., Ratsimba, B., 1996. Particle size determination by laser reflection: methodology and problems. Part. Part. Syst. Char. 13, 10–17.

Nilkumhang, S., Basit, A.W., 2009. The robustness and flexibility of an emulsion solvent evaporation method to prepare pH-responsive microparticles. Int. J. Pharm. 377, 135–141.

Qi, S., Marchaud, D., Craig, D.Q.M., 2010. An investigation into the mechanism of dissolution rate enhancement of poorly water-soluble drugs from spray chilled gelucire 50/13 microspheres. J. Pharm. Sci. 99, 262–274.

Richter, A., Voigt, T., Ripperger, S., 2007. Ultrasonic attenuation spectroscopy of emulsions with droplet sizes greater than 10 [mu]m. J. Colloid Interface Sci. 315, 482–492.

Ruf, A., Worlitschek, J., Mazzotti, M., 2000. Modeling and experimental analysis of PSD measurements through FBRM. Part. Part. Syst. Char. 17, 167–179.

Sansdrap, P., Moes, A.J., 1993. Influence of manufacturing parameters on the size characteristics and the release profiles of nifedipine from poly(D,L-lactide-co-glycolide) microspheres. Int. J. Pharm. 98, 157–164.

Scheler, S., 2011. Interpretation of FBRM signals by ray tracing, Joint Meeting of the Austrian and German Pharmaceutical Societies, September 20–23, 2011 , Innsbruck, Austria, http://www.uibk.ac.at/news/oephg-dphg2011/program/final-program-and-book-of-abstracts—joint-meeting-oephg-dphg-2011b.pdf.

Simmons, M.J.H., Langston, P.A., Burbidge, A.S., 1999. Particle and droplet size analysis from chord distributions. Powder Technol. 102, 75–83.

Sparks, R.G., Dobbs, C.L., 1993. The use of laser backscatter instrumentation for the online measurement of the particle-size distribution of emulsions. Part. Part. Syst. Char. 10, 279–289.

Tamilvanan, S., Sa, B., 1999. Effect of production variables on the physical characteristics of ibuprofen-loaded polystyrene microparticles. J. Microencapsul. 16, 411–418.

Turner, D.J., Miller, K.T., Sloan, E.D., 2009. Direct conversion of water droplets to methane hydrate in crude oil. Chem. Eng. Sci. 64, 5066–5072.

Worlitschek J., 2003. Monitoring, modeling and optimization of batch cooling crystallization. Dissertation, ETH Zürich.

Wynn, E.J.W., 2003. Relationship between particle-size and chord-length distributions in focused beam reflectance measurement: stability of direct inversion and weighting. Powder Technol. 133, 125–133.

Yeo, Y., Park, K.N., 2004. Control of encapsulation efficiency and initial burst in polymeric microparticle systems. Arch. Pharmacal Res. 27, 1–12.

Yu, W., Erickson, K., 2008. Chord length characterization using focused beam reflectance measurement probe – methodologies and pitfalls. Powder Technol. 185, 24–30.

Zidan, A.S., Ziyaur, R., Mansoor, A.K., 2010. Online monitoring of PLGA microparticles formation using Lasentec focused beam reflectance (FBRM) and particle video microscope (PVM). AAPS J. 12, 254–262.